Performance of Multidimensional Multicode DS-CDMA Using Code Diversity and Error Detection

Dong In Kim, *Member, IEEE,* and Vijay K. Bhargava, *Fellow, IEEE*

***Abstract*—High rate transmission can be realized using multiple orthogonal codes (MOC), as proposed in the third-generation wide-band code-division multiple-access (W-CDMA) standard. However, the linear sum of MOC channels is no longer constant amplitude, and a highly linear, power-inefficient amplifier may be required for transmission. Recently, a nonlinear block coding technique called precoding is introduced to maintain a constant amplitude signal after superposition of MOC channels. This is achieved by adding redundancy. In this paper, we first describe a multidimensional signaling scheme that recovers some information rate loss by precoding. Second, we propose a self-interference (SI) cancellation scheme resulting from a code diversity between the in-phase and quadrature subchannels among MOC channels. In a typical wireless channel with multipath fading, this type of SI can be detrimental especially when the number of parallel MOC channels is large. Third, we show that the error detection capability of precoding can be combined with code diversity, resulting in a diversity gain. In addition, we show that the diversity gain can be achieved using antenna diversity to assure the degree of freedom in code diversity, and even with the large number of MOC channels, the error performance can be maintained reliably while outperforming the variable spreading factor scheme in W-CDMA.**

***Index Terms*—Antenna diversity, code diversity, error detection, multicode DS-CDMA, multidimensional signaling, precoding, self-interference cancellation.**

I. Introduction

NECESSITY of high rate transmission is rapidly growing in the circle of wireless mobile communications. It is expected that the third-generation wideband CDMA (W-CDMA) system can be deployed in the near future to provide wireless multimedia services, but the rate is somewhat limited, for instance, up to the first phase rate of 384 kb/s. To achieve the specified rate, two types of approaches are being considered where one is the variable spreading factor (VSF) scheme using a single code [1], [2], and the other is a multicode direct-sequence CDMA (DS-CDMA) based on parallel MOC channels [3], [4].

Tradeoffs between the two schemes are as follows. The VSF scheme can adjust the spreading gain depending on the input traffics and control the power of signal to meet the quality of services (QoS), whereas the multicode scheme changes the number of code channels required at a specific rate to maintain a constant processing gain. From a complexity point of view, the latter has a certain disadvantage over the VSF scheme which requires only a single RAKE receiver. Thus, the use of multicode transmission is more suitable for uplink rather than downlink because the complexity is prohibitive for a mobile unit. However, the multicode scheme has a drawback of high envelope fluctuations as a result of a large linear sum of multicode signals. There have been a number of techniques to reduce such envelope fluctuations by inserting precoding [5], [6] before multicode signaling.

The precoding scheme may produce low envelope variations, but also causes a loss in the information rate which is highly undesirable for high rate data services. To overcome this, a multidimensional (MD) multicode signaling scheme was proposed in [7], in which the signaling is performed both in code and time spaces to fully exploit the resources in the modulation process. With the signaling,[1] the rate can be further increased by compensating such information rate loss by precoding. However, as the number of channels increases, we are faced with another drawback of the performance degradation incurred by precoding because the signal energy carried on precoding channels with no information is wasted. In general, wireless multimedia services require higher data rates and better link quality at the same time. Therefore, it is necessary for multicode signaling to prevent such loss in the signal energy when implementing a receiver with limited complexity. Fortunately, the precoding channels offer error detection capability to mitigate the degradation, and also the property of constant envelope allows an easy implementation of error detection scheme. In this paper, the feasibility of performance improvement by error detection is addressed.

On the other hand, wireless channels experience multipath fading impairment which often requires a diversity technique to mitigate an undue increase in the signal energy for a specific error rate. In particular, when high rate transmission is required for the multicode signaling, the self-interference (SI) caused by nonorthogonal delayed versions of a signal becomes more severe for a high rate user. As the number of channels increases, it is necessary for a multicode scheme to minimize the effect of SI on the error performance. In general, if we employ independent I/Q code sequences for quadrature phase-shift keying (QPSK) spreading, then the decision statistics after QPSK despreading become uncorrelated for the in-phase (I)/quadrature

Paper approved by J. Wang, the Editor for Equalization of the IEEE Communications Society. Manuscript received April 1, 2000; revised August 19, 2000 and October 1, 2000. This work was supported in part by the Research Fund of the University of Seoul, Seoul, Korea, and in part by the Natural Sciences and Engineering Research Council of Canada. This paper was presented in part at the 2000 IEEE Fourth CAS Workshop on Emerging Technologies in Circuits and Systems: Third Generation Mobile Technologies and Applications, Hong Kong, November 2000.

D. I. Kim is with the School of Electrical Engineering, University of Seoul, Seoul 130-743, Korea (e-mail: dikim@uoscc.uos.ac.kr).

V. K. Bhargava is with the Department of Electrical and Computer Engineering, University of Victoria, Victoria, BC V8W 3P6, Canada (e-mail: bhargava@ece.uvic.ca).

Publisher Item Identifier S 0090-6778(01)04079-X.

[1]Compared to conventional multicode signaling, the MD multicode signaling performs comparably or even better in terms of the symbol-error rate with increased data rate [7].

(Q) subchannels [8]. With no fading, symbol errors may occur randomly because of the independent I/Q scrambling process which in turn enables us to cancel the SI between the I/Q subchannels. If the I/Q subchannels are correlated due to complex spreading, for instance, it is hard to remove the SI because of correlated errors. The property that offers suppression of I/Q-subchannel SI will be referred to as *code diversity*. If we treat I/Q subchannels (or M parallel MOC channels) as separate users, we may apply approaches developed for multiuser detection [9] to this SI cancellation. But the receiver complexity caused by MD signaling is too high, and hence we focus on a simpler and effective realization of receiver based on the code diversity.

In fact, a signal suffers from correlated fading in an I/Q code-multiplexed channel which limits the degree of freedom[2] in code diversity; using code diversity alone therefore does not improve the error performance. To avoid the unfavorable situation, the impairment due to correlated fading should be mitigated by adopting antenna diversity commonly used in cellular environment [10], resulting in an enlarged degree of freedom. It is expected that the fade variations in the code-multiplexed channel can be normalized enough to assure code diversity with a certain gain. In addition, the error detection capability permits the receiver to be able to locate a deep fade and avoid unreliable code diversity; that is, to stop the SI cancellation during the period of deep fade. Its positive effect is more growing as the number of channels increases, so the code diversity combined with error detection is very effective in yielding better link quality even when high rate transmission is required.

The main purpose of this paper is to improve the error performance even for the large number of MOC channels to be required at high rates, while a constant envelope property is kept by the MD multicode signaling with precoding. For the latter, it is a prerequisite to employ a power-efficient and cost-effective nonlinear amplifier at the mobile unit. Tradeoff between having the constant envelope and loss in the signal energy is overcome by using code diversity and error detection. Also, one possible receiver for the uplink channel can be based on both the I/Q SI cancellation that results from code diversity and error detection.

In Section II, we will introduce a single-cell W-CDMA system which employs two different signal sets, MD multicode and conventional DS-CDMA, depending on the data rates. An algorithm on SI cancellation is described in Section III, along with a realization of error detection based on precoding channels. In Section IV, the improvement by code diversity and error detection is evaluated theoretically in terms of the symbol-error rate (SER). Numerical and simulation results are provided in Section V to see the error performance of the I/Q SI cancellation with error detection, and also compared with the VSF scheme in view of the bit-error rate (BER). Finally, concluding remarks are given in Section VI.

[2]The degree of freedom appears as one (normalized) in case of no fading, but with fading a signal attenuation reduces the degree of freedom, i.e., less than one.

II. Multidimensional W-CDMA System

A. Transmitter

We consider the uplink transmission that uses MD multicode signaling in [7] for high rate users and conventional DS-CDMA for low rate users. In general, the number of low rate users in the system is greater than that of high rate users, and it is assumed that a single high rate user coexists with $(K-1)$ interfering low rate users in a single-cell W-CDMA system. For low rate users, adaptive antenna array diversity [11] can be applied to reduce severe interference from high rate users. Hence, we focus on the high rate user subjected to the SI that grows in proportion to the number of MOC channels being used.

First, multicode signaling uses dual binary phase-shift keying (BPSK) for data modulation and QPSK for spreading, both of which are considered in W-CDMA uplink [2]. Then, MD signaling introduces additional G-ary orthogonal modulation for each set of J MOC channels where $G \triangleq N/M$, N is the number of chips per symbol and M is the total number of MOC channels. Therefore, the MD multicode signaling results in *biorthogonal* signaling which carries a maximum of $(M+M/J\log_2 G)$ information bits per symbol in the I or Q subchannel. Note that the MD multicode signaling can also be applied to both IS-95 and W-CDMA uplinks using only BPSK modulation with QPSK spreading/complex spreading, which are not considered here for code diversity. For compatibility with the above standards, we may consider the MD multicode DS-CDMA using antenna diversity rather than code diversity (see Fig. 8 for BER comparison with VSF) while the error detection capability may be used to properly remove the receive antenna with unreliable paths in diversity combining.

Second, the MD multicode signaling may adopt a source encoding in view of error protection, which maps two codewords with maximum Hamming distance into antipodal signals with same orthogonally modulated sequence, having the largest Euclidean distance. Then, all data bits are uniformly protected against the most probable errors because they have the same Euclidean distance. For instance, QPSK data modulation with Gray encoding, which is biorthogonal.

Third, the proposed signaling scheme is suitable for the uplink, and it is desired to have a constant envelope signal of amplitude $\sqrt{M}$ where precoding is adopted. The precoding in case of $M = 4, 16$ is fully described in [7].

In the uplink, the transmitted signal of a high rate (first) user can be expressed by

$$\begin{aligned} s(t) = \sum_{n=0}^{N_f-1}\sum_{g=0}^{G-1}\sum_{m=0}^{M-1} \sqrt{P}\,\big[d_{I,m}(n)b_{I,\langle m\rangle}(g;n) \\ \cdot c_I(t-gT_w-nT) + jd_{Q,m}(n)b_{Q,\langle m\rangle}(g;n) \\ \cdot c_Q(t-gT_w-nT)\big]\, w_m(t-gT_w-nT). \end{aligned} \quad (1)$$

In the above, P is the signal power per channel, $\{d_{O,m}(n), m = 0,1,\ldots,M-1\}$ represent the M parallel binary data of $O = I$ or Q subchannel at the nth signaling time, $\{b_{O,\langle m\rangle}(g;n), g = 0,1,\ldots,G-1\}$ are the modulating sequences for the $\langle m\rangle$th J channels where $\langle m\rangle \triangleq \lfloor m/J \rfloor$ for some integer $J > 1$ and $\lfloor x \rfloor$ equals the greatest integer not exceeding x, T_w and $T = GT_w$

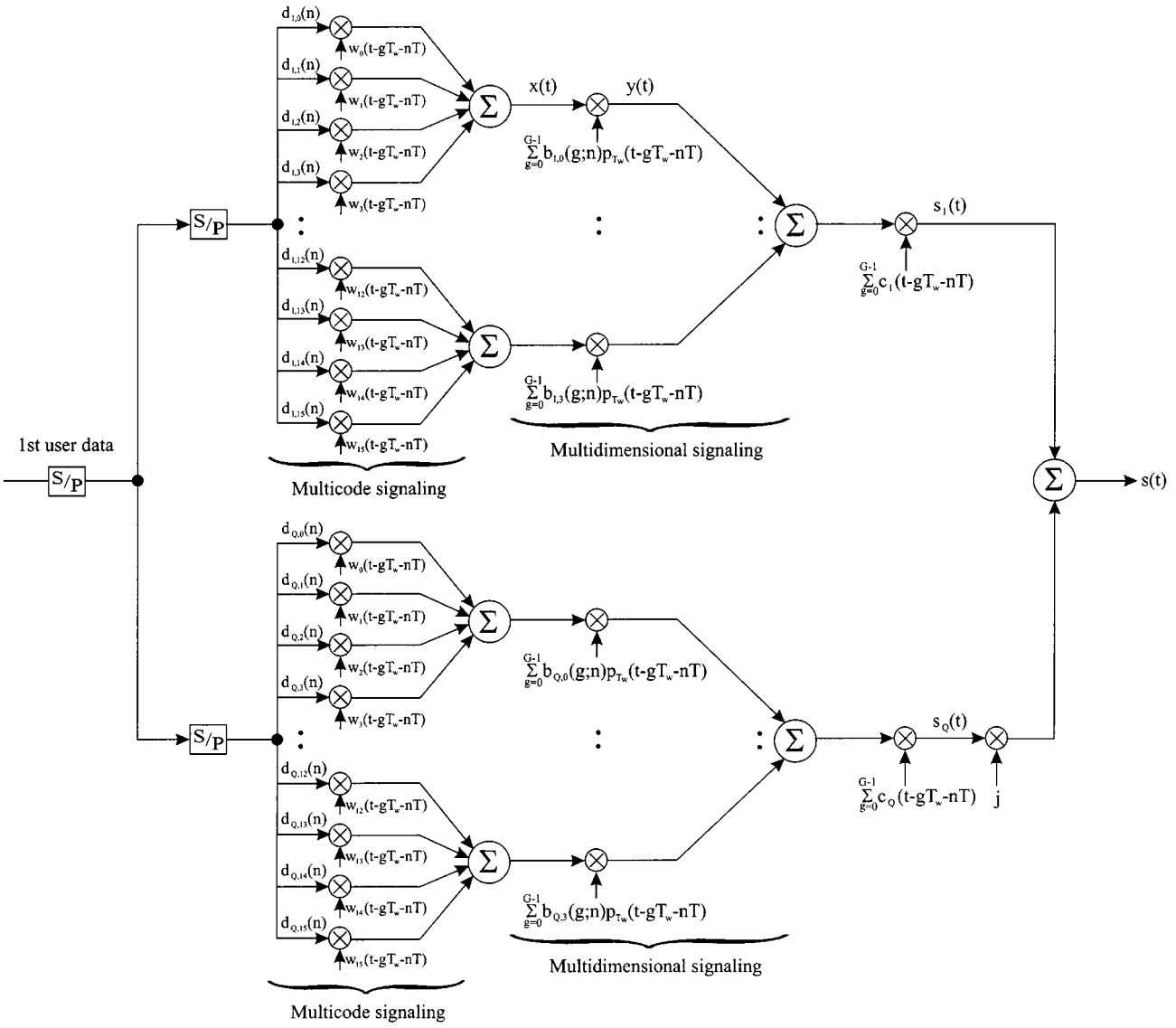

(a)

Fig. 1. MD multicode DS-CDMA signaling for a high rate user. (a) Block diagram $(M = 16, J = 4)$.

denote the Walsh and data symbol times, respectively, and N_f is the frame length.

In addition, the Walsh symbol $w_m(t), m = 0, 1, \ldots, M-1$, is defined by

$$w_m(t) = \sum_{l=0}^{M-1} w_{m,l} p(t - lT_c) \tag{2}$$

where $p(t)$ is a rectangular chip waveform occupied in $[0, T_c)$ with unit magnitude and a chip time T_c, and $\mathbf{w}_m = (w_{m,0}, w_{m,1}, \ldots, w_{m,M-1})$ is chosen from the mth row vector of Hadamard matrix, H_M $(M \times M)$ with elements ± 1. To provide code diversity between the I and Q subchannels, we introduce independent I/Q spreading, namely

$$c_O(t - gT_w - nT) = \sum_{l=0}^{M-1} c_{O,nN+gM+l} p(t - (nN + gM + l)T_c) \tag{3}$$

for $O = I, Q$ and $T_c = T/N = T_w/M$ $(N = GM)$. We assume that $\{c_{O,l}, l = 0, 1, \ldots\}$ are statistically independent for the I and Q subchannels because of distinct long pseudonoise (PN) sequences.

A W-CDMA transmitter for the high rate user is illustrated in Fig. 1(a) when $M = 16$ and $J = 4$, where $p_{T_w}(t)$ is a rectangular pulse waveform in $[0, T_w = MT_c)$. For instance, if we are using only $M = J = 4$ MOC channels, then the resulting waveforms can be shown in Fig. 1(b). It is noted that the modulating sequences $\{b_{O,\langle m \rangle}(g; n), g = 0, 1, \ldots, G-1\}$ can send additional L $(\leq \log_2 G)$ information bits, resulting in a total of $(M + LM/J)$ bits per N chips.

Here, the $(K-1)$ low rate users that cause the multiple-access interference (MAI) are equivalently modeled as

$$s_k(t) = \sum_{l=0}^{NN_f} \sqrt{P_k} \left[a_{I,l}^{(k)} + j a_{Q,l}^{(k)} \right] p(t - lT_c), \quad k = 2, \ldots, K \tag{4}$$

For instance ;

$d_{1,0}(n) = d_{1,1}(n) = d_{1,2}(n) = 1,\ d_{1,3}(n) = -1\ ;\ \{b_{1,0}(g;n) \mid g = 0,1,2,3\} = (1,-1,-1,1)$

$H_4 = [w_{m,\ell}]\ ,\quad \{c_{1,\ell}\} = (1, -1, 1, -1, 1, 1, -1, -1, 1, -1, -1, -1, 1, 1, 1, -1)$

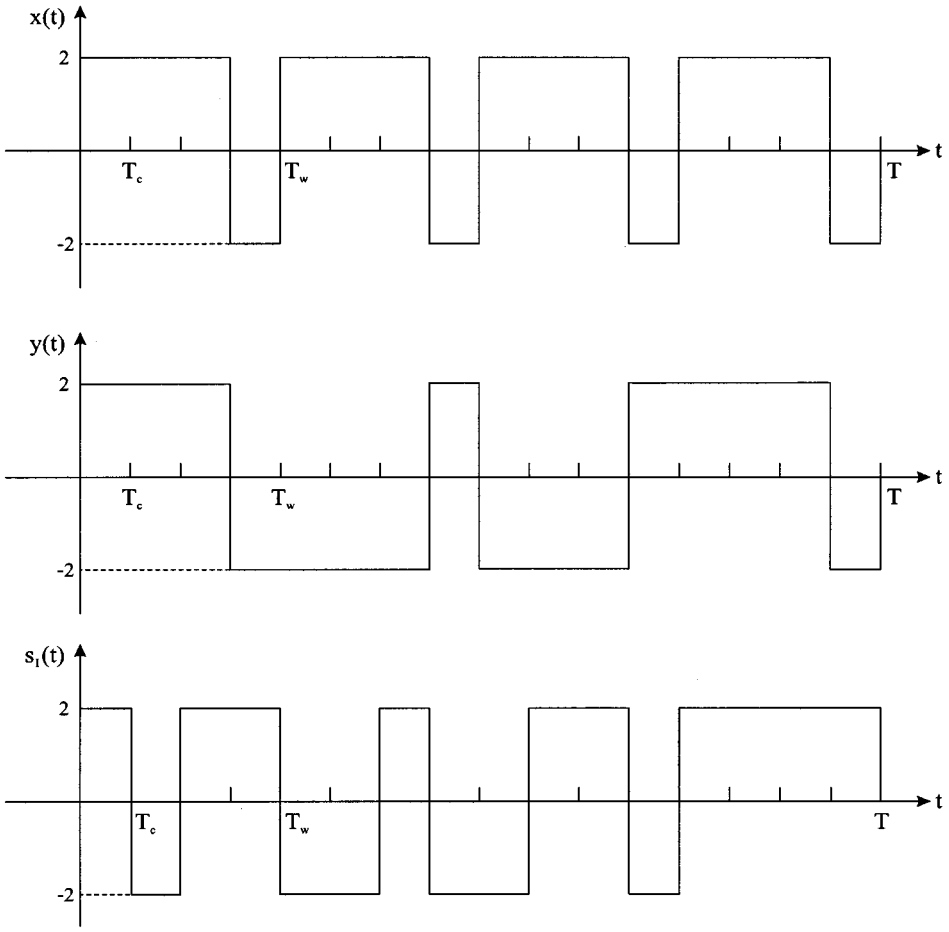

(b)

Fig. 1. *(Continued.)* MD multicode DS-CDMA signaling for a high rate user. (b) Waveforms $(M = J = 4, G = 4, N = 16)$.

in which P_k is the kth user's signal power, and $\{a_{O,l}^{(k)}, l = 0, 1, \ldots\}$ are assumed to be random binary sequences for chip-by-chip independence. Note that the bit energy is set to $E_b = P_k N_k T_c$ and then N_k will determine the bit rate of the kth low rate user.

For comparison, if the high rate user uses the VSF scheme using a single code [2], $s(t)$ in (1) is rewritten as

$$s(t) = \sum_{n=0}^{N_f R-1} \sqrt{P_b}\,[d_{I,n} c_I(t - nT_b) + j d_{Q,n} c_Q(t - nT_b)] \tag{5}$$

where the data rate is $R = (M + LM/J)$, $E_b = P_b T_b$ for $T_b = T/R$ and

$$c_O(t - nT_b) = \sum_{l=0}^{N_b-1} c_{O,l+nN_b} p(t - (l + nN_b)T_c) \tag{6}$$

for $O = I, Q$ and $N_b = T_b/T_c$. Here, we assume that the signal energy $E = PT$ per channel in (1) is related to the bit energy E_b using $E = RE_b/M$.

For the VSF scheme, the complex spreading [2] used in W-CDMA may be inserted to achieve low envelope variations, but here we do not consider bandlimiting and only the signal amplitude characteristics are considered. In addition, when distinct spreading codes of long period are used, the SI due to nonorthogonal delayed signals remains almost the same even with the complex spreading/despreading. On the other hand, $(K - 1)$ low rate users generate the MAI where the signal in (4) is modeled as random binary sequences and the complex despreading will not change the MAI statistics.

B. Channel

The channel experiences a multipath fading with different delays $\{\tau_{k,v}, k = 1, \ldots, K; v = 1, \ldots, V\}$ when V paths are present. Then, the MD W-CDMA signal causes the SI among

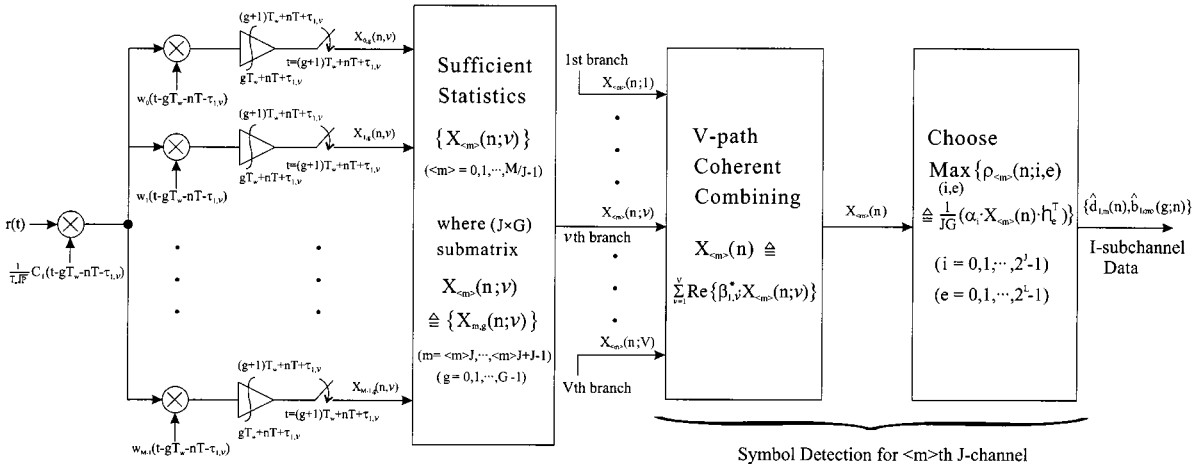

Fig. 2. Symbol-by-symbol detection of J-channel MD multicode signals.

M parallel MOC channels due to its nonorthogonal delayed signals. The signals are also affected by their individual path gains, $\{\beta_{k,v}, k = 1,\ldots,K; v = 1,\ldots,V\}$, which can be modeled as complex-valued Gaussian random variables, namely, Rayleigh-faded gains. Hence, a low-pass equivalent channel impulse response is given by

$$h_k(t) = \sum_{v=1}^{V} \beta_{k,v}\delta(t - \tau_{k,v}) \tag{7}$$

for the kth user link at a central receiver, where $\{\tau_{k,v}\}$ are assumed to be uniformly distributed over $[0, T)$.

C. Receiver

To begin with, we assume no SI canceller (SIC) and no error detection at the central receiver. To properly detect the MD W-CDMA signal, therefore, we need to use a symbol-by-symbol detection based on the filtered output statistics of J parallel MOC channels, instead of a bit-by-bit detection. One possible receiver using the symbol detection may be realized as shown in Fig. 2, where the sufficient statistics $\{X_{\langle m\rangle}(n;v) \,|\, \langle m\rangle = 0,1,\ldots,M/J-1\}$ of the vth path are generated as follows.

First, the filtered output signal $X_{m,g}(n;v)$ associated with mth code channel, gth Walsh symbol, and nth signaling time at the vth path is

$$\begin{aligned} X_{m,g}(n;v) = \frac{1}{T_w\sqrt{P}} \int_{gT_w+nT+\tau_{1,v}}^{(g+1)T_w+nT+\tau_{1,v}} & r(t) \\ & \cdot c_I(t - gT_w - nT - \tau_{1,v}) \\ & \cdot w_m(t - gT_w - nT - \tau_{1,v})\, dt \end{aligned} \tag{8}$$

where $m = 0,\ldots,M-1$; $g = 0,\ldots,G-1$, and the received signal has the expression

$$r(t) = s(t) \otimes h_1(t) + \sum_{k=2}^{K} [s_k(t) \otimes h_k(t)] \tag{9}$$

$\otimes$ denoting the convolution. It is noted that the SI at the vth path is defined by

$$\begin{aligned} \mathrm{SI}_v &\triangleq \sum_{\substack{v'=1 \\ v'\neq v}}^{V} \beta_{1,v'}\, s(t - \tau_{1,v'}), \\ & t \in [gT_w + nT + \tau_{1,v}, (g+1)T_w + nT + \tau_{1,v}) \end{aligned}$$

where $\mathrm{SI}_v = \mathrm{SI}_v^{(I)} + j\,\mathrm{SI}_v^{(Q)}$, each due to the I and Q subchannels. Then, the submatrix $X_{\langle m\rangle}(n;v)$ is formed with elements $\{X_{m,g}(n;v) \,|\, m = \langle m\rangle J,\ldots,\langle m\rangle J+J-1; g = 0,\ldots,G-1\}$.

Now, performing V-path coherent combining and taking the real part yields the decision statistics $X_{\langle m\rangle}(n)$ in the I-subchannel

$$X_{\langle m\rangle}(n) = \sum_{v=1}^{V} \mathrm{Re}\left\{\beta_{1,v}^{*} X_{\langle m\rangle}(n;v)\right\} \tag{10}$$

$*$ denoting the complex conjugate. Note that with $c_Q(t)$ in (8), taking the imaginary part in (10) yields the decision statistics in the Q-subchannel. Finally, a symbol-by-symbol detection will be made by applying the decision rule, that is, choose

$$\max_{\substack{(i=0,\ldots,2^J-1) \\ (e=0,\ldots,2^L-1)}} \left\{\rho_{\langle m\rangle}(n;i,e) = \frac{1}{JG}\left(\alpha_i \cdot X_{\langle m\rangle}(n) \cdot \mathbf{h}_e^T\right)\right\} \tag{11}$$

where the symbol α_i is an J-tuple row vector with elements ± 1 and $\mathbf{h}_e$ denotes the modulating sequence with size G and elements ± 1, for instance, the eth row vector of Hadamard matrix H_G $(G \times G)$ with elements ± 1.

Meanwhile, we assume a bit-by-bit detection and a single RAKE combining for the VSF scheme, resulting in simplified receiver structure.

III. Self-Interference Canceller with Error Detection

The performance of a symbol-by-symbol detection is somewhat degraded due to the SI among M parallel MOC channels under the multipath fading. In particular, as the number of MOC channels increases, the effect would be more prominent and hence the MD signaling should be combined with a certain

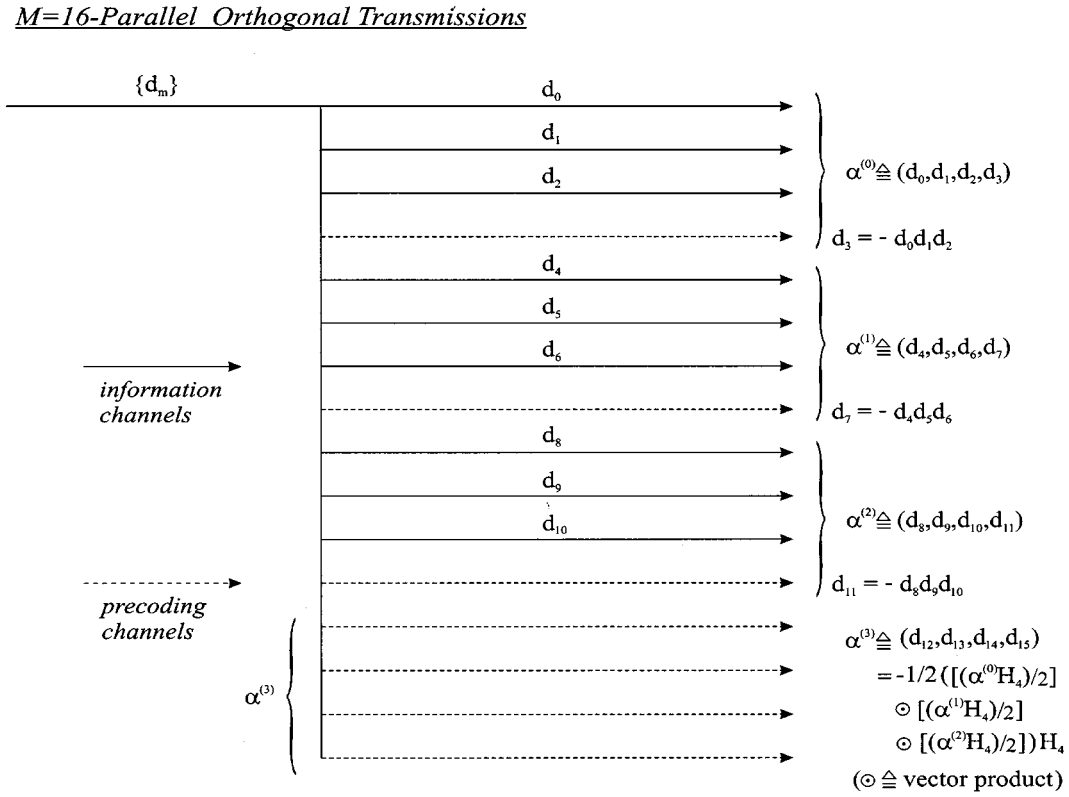

Fig. 3. Precoding for a constant envelope multicode signal when $M = 16$ and $J = 4$.

type of SIC. For this reason, we propose a new SIC which exploits code diversity between the I and Q subchannels, resulting from independent I/Q spreading. With the long PN sequences, varying from symbol to symbol, the two subchannels are statistically uncorrelated and become independent when the Gaussian assumption on interference is invoked.

For possible theoretical analysis, a separate pilot channel is assumed, but the pilot symbols can be code-multiplexed into Q subchannel together with part of data symbols, like W-CDMA uplink [2] when multicode transmission is used. In this case, the MD multicode signaling should consider the power allocation to the pilot symbols for a constant envelope signal, which prohibits theoretical analysis for QPSK spreading. Thus, more detailed analysis on this and the effect of SI to and from pilot symbols should be further studied.

Based on the above observations, the proposed algorithm for the cancellation of the SI between the I and Q subchannels is described as follows.

1) An initial symbol-by-symbol detection is made on the I/Q-subchannel data stream.
2) Eliminate the SIs $\{\mathrm{SI}_v^{(I)}, \mathrm{SI}_v^{(Q)}\}$, $v = 1, \ldots, V$ caused by the I/Q-subchannel delayed signals using initial estimates,[3] and then perform a symbol-by-symbol detection on the I/Q-subchannel data stream.
3) Eliminate the SIs $\{\mathrm{SI}_v^{(I)}, \mathrm{SI}_v^{(Q)}\}$, $v = 1, \ldots, V$ using the second estimates, and perform a symbol-by-symbol detection on the I/Q-subchannel data stream.

[3]The estimates on path gains $\{\beta_{1,v}\}$ and delays $\{\tau_{1,v}\}$ are assumed to be available by the use of a separate pilot channel in the uplink.

It is expected that further iteration of this algorithm would not result in any improvement in error performance.

On the other hand, if we adopt precoding [6] to have a constant envelope signal in the MD signaling, there are some number of precoding channels that convey data with no information as shown in Fig. 3. A symbol-by-symbol detection when $M = J = 4$ uses all signal energy including the signal energy of d_3 carried on the precoding channel. But, when $M = 16$, there is a separate data symbol $\alpha^{(3)}$ conveyed on the four parallel precoding channels whose signal energy is not used at the symbol-by-symbol detection with $J = 4$. Thus, we may have some performance degradation incurred by such loss in the signal energy, which will make it difficult to achieve high data rates with $M = 16$, while maintaining the link quality reliably. To avoid this, the error detection capability of precoding may be combined with the I/Q SIC. The proposed algorithm is then nicely refined as follows.

1) The SI cancellation is performed for the corresponding I/Q subchannels only when the other subchannel contains no symbol error in a given time.
2) A symbol-by-symbol detection is selectively made on the I/Q-subchannel data stream only if initial errors have been detected in the corresponding channels.

Fig. 4 illustrates the proposed I/Q SI cancellation combined with error detection and provides initial estimates. Here, errors can be easily detected by checking the constant envelope of $\{s_I(t), s_Q(t)\}$ in the I/Q subchannels where the complex envelope is given by $s(t) = s_I(t) + js_Q(t)$. The SIs are related to $\mathrm{SI}_v^{(O)} = \sum_{\substack{v'=1 \\ v' \neq v}}^{V} \beta_{1,v'} s_O(t - \tau_{1,v'})$ $(O = I, Q)$.

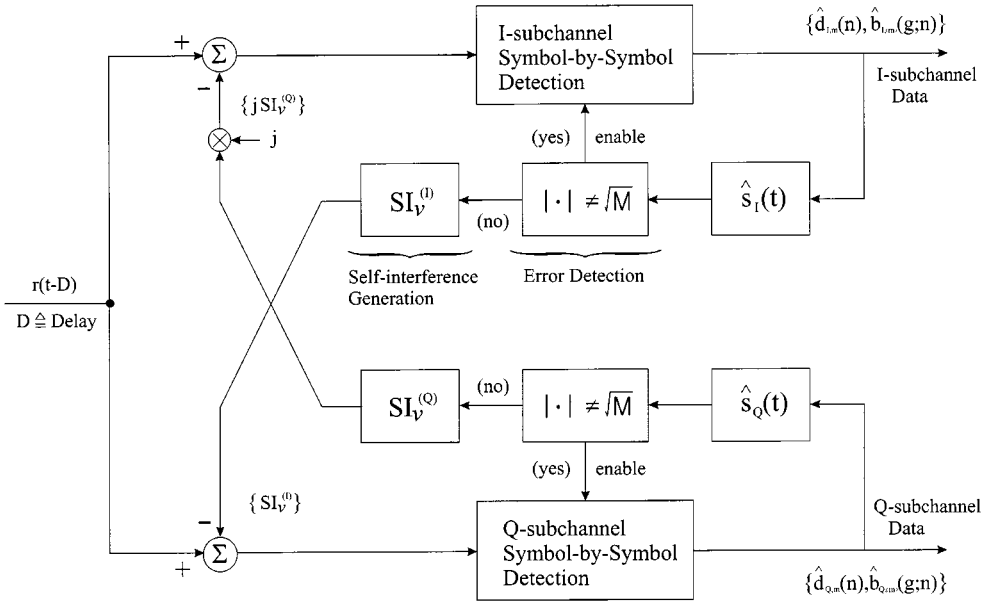

Fig. 4. Receiver structure with I/Q SI cancellation and error detection.

IV. Analysis of Error Performance

The error performance of MD W-CDMA system is derived through the probability of symbol error based on each J MOC channels. Here, a channel is classified as multipath with Rayleigh fading that causes the SI due to delayed versions of a signal. In particular, it is effective for MD signaling to null the effect of SI on the error performance. This is because the signaling is based on M parallel transmissions and so intersymbol interference can be confined to two adjacent symbols.

For the proposed SIC with $M = 4$, a correct cancellation in one channel will occur when two adjacent symbols causing the SI are correctly decided in the other channel. First, suppose α_i and $\mathbf{h}_e$ were sent, then the decision variable $\rho_{\langle m\rangle}(n;i,e)$ in (11) is expressed by

$$\rho_{\langle m\rangle}(n;i,e) = \sum_{v=1}^{V}|\beta_{1,v}|^2 + \sum_{k=2}^{K}\mathrm{MAI}_k(i,e) + \sum_{v=1}^{V}\left[\mathrm{MAI}_{1,v}^{(I)}(i,e) + \mathrm{MAI}_{1,v}^{(Q)}(i,e)\right] \quad (12)$$

where the second and third terms represent the other-user interference and the I/Q-subchannel SI, respectively. Once the SI is correctly eliminated using decisions on two adjacent symbols in the Q subchannel, then the decision variable becomes $\rho_{\langle m\rangle}(n;i,e) = \sum_{v=1}^{V}|\beta_{1,v}|^2 + \sum_{k=2}^{K}\mathrm{MAI}_k(i,e) + \sum_{v=1}^{V}\mathrm{MAI}_{1,v}^{(I)}(i,e)$. But, if the two symbols are decided incorrectly, the effect of the resulting SI is equivalent to the SI, $\sum_{v=1}^{V}[\mathrm{MAI}_{1,v}^{(I)}(i,e) + \sqrt{2}\mathrm{MAI}_{1,v}^{(Q)}(i,e)]$ in the mean-square sense, referring to Appendix A.

For analysis, we derive a meaningful result for the error performance by using a first-order approximation, that is, by assuming that two adjacent symbol errors are highly correlated due to fading and correlated interferences. Hence, a symbol-error event simply assures an incorrect SI cancellation and, likewise, a correct SI cancellation results from no symbol error. Based on these facts, the error performance at the first SIC is of the form

$$P_1(\epsilon) \cong P(\epsilon\,|\,S)\cdot[1 - P(\epsilon)] + P(\epsilon\,|\,\bar{S})\cdot P(\epsilon) \quad (13)$$

where the event S indicates a correct SI cancellation with its complement $\bar{S}$ and the subscript 1 represents the first iteration.

First, the initial decision error measured by $P(\epsilon)$ is derived for Gaussian-modeled interference because a relatively large K is considered and the central limit theorem works well for multipath-induced interference. Since α_i is antipodal, so that the MD signaling here forms a biorthogonal signal set [12], we find that

$$P(\epsilon) = 1 - \Pr\left[\bigcap_{(i',e')\neq(i,e)}\left|\rho_{\langle m\rangle}(n;i',e')\right| < \rho_{\langle m\rangle}(n;i,e)\,\middle|\,\alpha_i,\mathbf{h}_e\right] \quad (14)$$

for $i = 0,1,\ldots,2^{J-2}-1$ and $e = 0,1,\ldots,2^L-1$. Here, we have used that $|\{\alpha_i\}| = 2^{J-1}$ due to 1-bit precoding. Let us define $Y(i,e) = \sum_{k=2}^{K}\mathrm{MAI}_k(i,e) + \sum_{v=1}^{V}[\mathrm{MAI}_{1,v}^{(I)}(i,e) + \mathrm{MAI}_{1,v}^{(Q)}(i,e)]$, where the probability density function of $Y(i,e)$ is $1/\sigma_I\phi(y/\sigma_I)$ for $\phi(x) = 1/\sqrt{2\pi}\exp(-x^2/2)$ and $\sigma_I^2 = \mathbf{E}\{Y(i,e)^2\}$, $\mathbf{E}$ denoting the expectation. In Appendix A, it is shown that $\{\rho_{\langle m\rangle}(n;i,e)\}$ become mutually independent because of orthogonality where uncorrelated scattering and equal average path power are assumed. Therefore, it can be simplified to

$$P(\epsilon) = 1 - \int_0^{\infty}[1 - 2Q(x)]^{2^{J+L-2}-1}\phi(x-\sqrt{\gamma})\,dx \quad (15)$$

where $Q(x) = \int_x^\infty \phi(u)\,du$, and the output *per-symbol* signal-to-interference ratio (SIR) is shown in Appendix A to be

$$\gamma = \left(\frac{\sum_{v=1}^{V}|\beta_{1,v}|^2}{\sigma_\beta^2}\right) \cdot \left[\frac{JN}{2[(K-1)V\varepsilon^2 + M(V-1)]\mathbf{E}\{\bar{\eta}^2(\delta)\}}\right] \quad (16)$$

for $\sigma_\beta^2 = \mathbf{E}\{|\beta_{k,v}|^2\}$ and $\varepsilon^2 \triangleq P_k/P$ $(k \geq 2)$. Here, the partial chip-pulse correlation is $\bar{\eta}(\delta) = 1/T_c \int_0^\delta p(t)p(t-\delta+T_c)\,dt$, where δ is uniformly distributed over $[0, T_c)$. It is noted that *per-symbol* is equivalent to the $(J-1+L)$ information bits conveyed on each J MOC channels.

Based on the initial measure $P(\epsilon)$, the SIC's performance measures $P(\epsilon\,|\,S)$ and $P(\epsilon\,|\,\bar{S})$ in (13) can be derived by replacing the *per-symbol* SIR γ in (15) with

$$\gamma_- = \gamma(M \to M/2) \qquad \text{for the event } S \quad (17)$$

$$\gamma_+ = \gamma(M \to 3M/2) \qquad \text{for the event } \bar{S}. \quad (18)$$

The first iteration of SIC will then achieve the error performance $P_1(\epsilon)$ in (13) by substituting $P(\epsilon)$, $P(\epsilon\,|\,S)$, and $P(\epsilon\,|\,\bar{S})$. It should be averaged over γ for a realistic error performance, but its statistics are a complicated function of correlated fading and order of antenna diversity used, even with the multiple integrations involved. Due to computational difficulty, the ideal error performance offered by the SIC is evaluated theoretically through the average *per-symbol* SIR, $\bar{\gamma} = \mathbf{E}\{\gamma\}$, instead of γ in (15).

Next, consider the second iteration of SIC that has a more complicated error performance because the decision error here is correlated with the initial decision error, unlike independence at the first iteration in (13). In this case, the following proposition may be useful in deriving the error performance at the second iteration.

Proposition 1: Conditioned on decisions at the first iteration, the joint probabilities on initial and second-iteration decisions, mutually correlated, are defined and derived as

$$\begin{aligned} P(\epsilon \to c\,|\,S) &\triangleq \Pr[\text{initial decision error, correct second-iteration decision}\,|\,S] \\ &= P(c\,|\,S) - P(c \to c\,|\,S) \end{aligned} \quad (19)$$

$$\begin{aligned} P(c \to \epsilon\,|\,\bar{S}) &\triangleq \Pr[\text{correct initial decision, second-iteration decision error}\,|\,\bar{S}] \\ &= P(c) - P(c \to c\,|\,\bar{S}) \end{aligned} \quad (20)$$

where the event S indicates a correct SI cancellation with its complement $\bar{S}$ at the second iteration, $P(c) = 1 - P(\epsilon)$, $P(c\,|\,S) = 1 - P(\epsilon\,|\,S)$, and

$$P(c \to c\,|\,S_\pm) = \int_0^\infty \int_0^\infty [\Omega_\pm(x,y)]^{2^{J+L-2}-1} \cdot \phi(y - \psi_\pm x)\phi(x - \sqrt{\gamma_\pm})\,dx\,dy \quad (21)$$

for $S_- = S, S_+ = \bar{S}, \Omega_\pm(x,y) = \int_0^x 2\phi(z)[1 - Q(y+\psi_\pm z) - Q(y-\psi_\pm z)]dz$, and $\psi_\pm = [(3\pm1)/2 + 2(K-1)V\varepsilon^2/(M(V-1))]^{1/2}$.

Proof of Proposition 1: See Appendix B. □

Proposition 2: The error performance at the second SIC is closely approximated as

$$\begin{aligned} P_2(\epsilon) \cong\ & P(\epsilon) - P(\epsilon \to c\,|\,S)\cdot[1 - P(\epsilon\,|\,\bar{S})] \\ & - P(\epsilon \to c\,|\,\bar{S})\cdot P(\epsilon\,|\,\bar{S}) + P(c \to \epsilon\,|\,S) \\ & \cdot [1 - P(\epsilon\,|\,S)] + P(c \to \epsilon\,|\,\bar{S})\cdot P(\epsilon\,|\,S), \end{aligned} \quad (22)$$

where $P(\epsilon \to c\,|\,\bar{S}) = P(c\,|\,\bar{S}) - P(c \to c\,|\,\bar{S})$ and $P(c \to \epsilon\,|\,S) = P(c) - P(c \to c\,|\,S)$ for $P(c\,|\,\bar{S}) = 1 - P(\epsilon\,|\,\bar{S})$.

Proof of Proposition 2: See Appendix C. □

Meanwhile, if the precoding is introduced for $M = 16$, we may further reduce the error performances $P_i(\epsilon)$ $(i = 1, 2)$ by combining the error detection capability with the above SIC. For $J = 4$ and $M/J = 4$ in Fig. 3, the probability of error being detected is given by

$$\Pr[E] = 1 - [1 - P(\epsilon)]^4 \quad (23)$$

provided the undetected error event is ignored. Therefore, the error performance $P_1(\epsilon)$ will be approximated by

$$P_1(\epsilon) \cong P(\epsilon)\cdot\Pr[E] + P(\epsilon\,|\,S)\cdot\{1 - \Pr[E]\}. \quad (24)$$

Following Proposition 2, the error performance $P_2(\epsilon)$ at the second iteration is well approximated as

$$P_2(\epsilon) \cong P(\epsilon) - P(\epsilon \to c\,|\,S)\cdot\{1 - \Pr[E]\} \quad (25)$$

which shows an improvement by the error detection capability.

V. Results

The error performances such as $P(\epsilon)$, $P_1(\epsilon)$, and $P_2(\epsilon)$ are evaluated in the I/Q code-multiplexed channel for a high rate user with constant envelope MD signals [7] when $M = 4, 16$ and $J = 4$. Code diversity is achieved by adopting two spreading codes whose generator polynomials are given by $g_1(x) = x^{32} + x^{22} + x^2 + x + 1$ and $g_2(x) = x^{32} + x^{31} + x^{30} + x^{10} + 1$ [13]. The data rates are set to three different values, namely, lower rate with 1 bit per $N_k = 128$ chips, higher rates with 8 and 18 bits[4] per $N = 128$ chips, where the higher rates can be offered by the use of MD signals with $M = 4, L = 5$ and $M = 16, L = 3$, assuming $L = \log_2(N/M)$. For instance, the rates are equivalent to 8 kb/s for $(K-1)$ low rate users (interferers), 64 and 144 kb/s for a high rate user (desired). Here, the power ratio $\varepsilon^2 \triangleq P_k/P$ $(k \geq 2)$ can be set to the values $\varepsilon^2 = 1/2, 8/9$ $(M = 4, 16)$ because $P_k = MP/R$ at the rates $R = 8, 18$ bits per fixed $N_k = N = 128$ chips. It is assumed that the signal power P per channel is perfectly estimated, the delay spread of $N = 128$ chips and Doppler frequency of 80 Hz at the low rate of 8 kb/s.

Theoretical results are shown in Figs. 5 and 6 for varying K when $M = 4, 16$ are used, respectively. Note that the average output *per-symbol* SIR $\bar{\gamma}$ was used, and hence an ideal multipath channel with no fade variation was assumed. The SI caused by

[4]When $M = 16$ and $J = 4$, MD signaling is used for each set of $J = 4$ channels for the first 12 channels, while the last four channels are used only for precoding [7]. Thus, MD signaling carries a total of $3 \times 3 = 9$ information bits while multicode signaling carries 9 bits, resulting in a total of 18 bits per 128 chips.

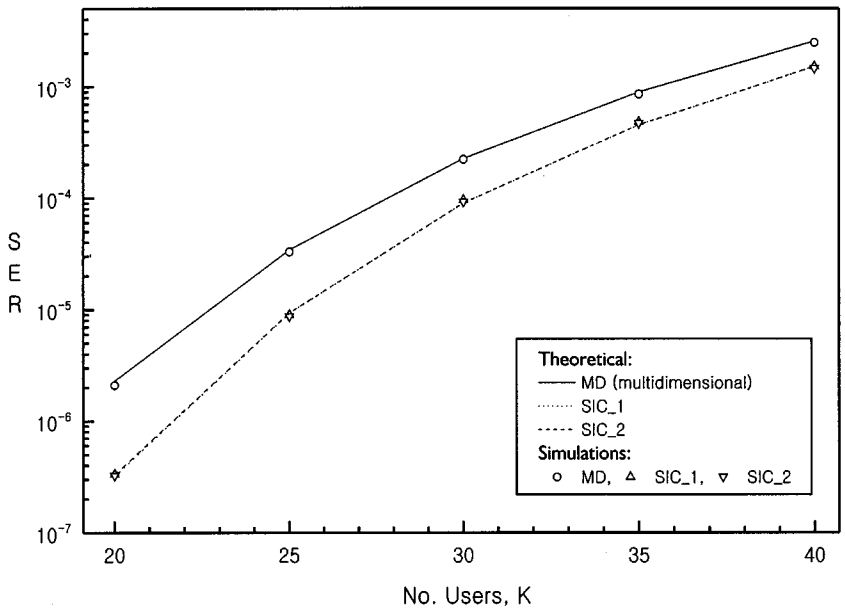

Fig. 5. SERs versus K when $M = 4$, $N = N_k = 128$, $G = 32$ and $L = 5$, assuming three-path coherent combining.

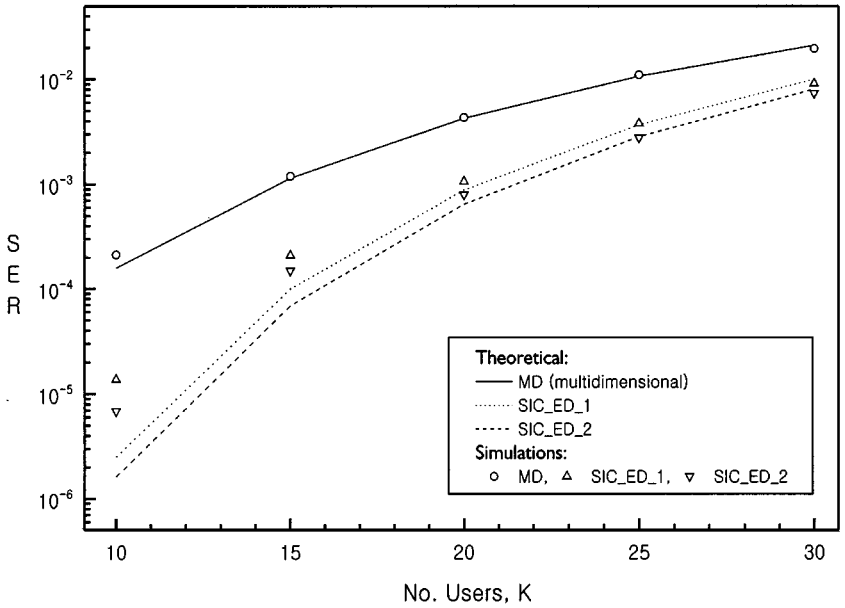

Fig. 6. SERs versus K when $M = 16$, $N = N_k = 128$, $G = 8$ and $L = 3$, assuming three-path coherent combining.

two delayed paths was taken into account so that a multipath of $V = 3$ was assumed. We see that theoretical results fit the simulation results, which assures validity of the first-order approximation to $P_i(\epsilon)$ $(i = 1, 2)$ in the analysis of error performance. It is also observed that the error performances are saturated at the second iteration, because the error events are statistically correlated at initial and second iterations (the index $i = 1, 2$ denote iteration for the SIC_i and SIC_ED_i in Figs. 5–8). Especially, the error detection capability provides a certain diversity gain while a noisy SIC in case of $M = 4$ may limit the gain in code diversity. It should be pointed out that if the effect of other-user interference can be diminished—for instance, adopting the multiuser detector [9]—the combined SIC and error detection (SIC_ED) scheme may be able to achieve its maximum diversity gain effectively in the region of smaller K. In fact, the MAI is more severe than the SI, and the proposed SIC_ED scheme for high rate users can be used efficiently in combination with some techniques to suppress the MAI. The Gaussian approximation is shown in Fig. 6 to be somewhat optimistic for smaller K [14] when compared to simulation results.

To look into a real diversity gain, a two antenna diversity scheme is adopted at the central receiver, like a base station, in order to mitigate the fade variations. Equal average path gain is assumed with uncorrelated scattering, and three-path coherent combining that results from two antenna branches is used to assure sufficient output *per-symbol* SIR γ. The error performances as a function of K are shown in Fig. 7 when $M = 16$. Compared to the ideal diversity gain, the performance improvement resulting from the combined SIC_ED is far reduced because correlated fading may cause the error events to be correlated in the

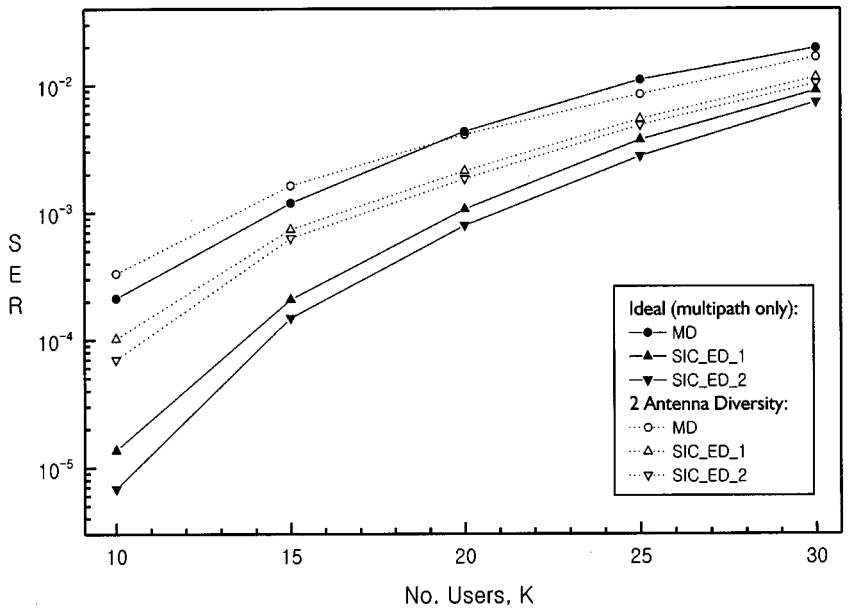

Fig. 7. SERs versus K when $M = 16$, $N = N_k = 128$, $G = 8$ and $L = 3$, assuming three-path/2 antenna diversity combining.

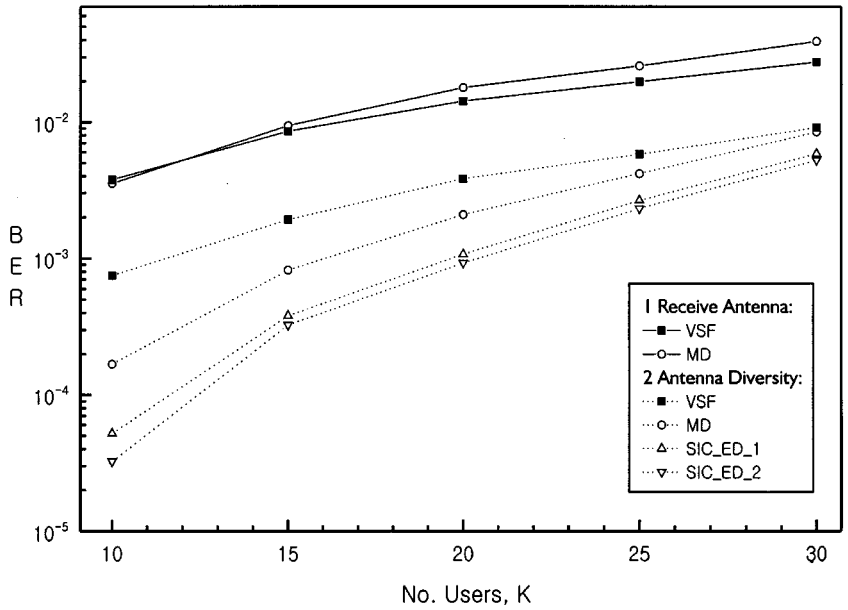

Fig. 8. BERs versus K when $M = 16$, $N = N_k = 128$, $G = 8$ and $L = 3$, assuming three-path/2 antenna diversity combining.

I/Q code-multiplexed channel. This implies that more antenna diversity should be adopted to fully exploit a certain diversity gain, while multiple antennas at both the base and remote stations are considered to increase the data rate [15]. As K increases, two antenna diversity performs well because of a capacity increase in interference-limited system [10].

Finally, the combined SIC_ED scheme is compared with the VSF scheme using a single code, both for a high rate user in view of the BER. Note that the SIC_ED is only considered for the MD multicode scheme using independent I/Q spreading because code diversity is not valid for complex spreading. To maintain the data rate almost the same for two schemes, an integer value $N_b = 8$ is selected to have the rate of $R = 16$ bits per $N = 128$ chips but $M = 16, L = 3$ gives the rate of $R = 18$ bits per $N = 128$ chips. For instance, the rate 128 kb/s can be supported by the VSF scheme, given 8 kb/s for a low rate user, while the rate 144 kb/s with the MD multicode DS-CDMA, conveying additional 16 kb/s. Even with higher rate, the combined SIC_ED scheme provides significant gain over the VSF scheme that is under consideration for high rate transmission in W-CDMA [2]. However, it should be pointed out that the proposed scheme requires a 6-bit (symbol) detection like IS-95 and $J = 4$ parallel RAKE receivers when $M = 16$ and $L = 3$, while the VSF scheme uses only a bit detection and a single RAKE receiver, resulting in much lower receiver complexity. Besides, when there is only one receive antenna with no SIC_ED, the results here and in [7] show that the proposed scheme with $M = 4$ performs better than the VSF scheme, whereas for large $M = 16$, the VSF scheme is comparable to the proposed scheme or even slightly better. This is because MD signaling is more sensitive

to fading, and precoding for constant envelope causes a loss in the signal energy.

Based on these facts, if more than two antenna diversity can be deployed at the base station and the MAI can be minimized by employing the multiuser detector, it is expected that the gain of code diversity will be maximized to offer higher data rates with large M.

VI. Conclusions

An MD multicode DS-CDMA has been applied to provide a certain diversity in the I/Q code-multiplexed channel, which enables us to increase the data rate with a large number of parallel MOC channels. The increased data rate results from the cancellation of SI among MOC channels by using code diversity because error patterns may occur in different manner due to independent I/Q spreading. Correlated fading, however, limits the degree of freedom in code diversity, resulting in far reduced diversity gain. To avoid this, the error detection capability of precoding has been utilized simultaneously with antenna diversity to lower the fade variations.

Through analysis and simulations, it was first observed that the ideal diversity gain, namely, taking into account only multipath, can be made sufficiently large by using both code diversity and error detection. Second, if the other-user interference can be maintained small, the gain that results will be fully exploited. Even faced with correlated fading, we found that, although the diversity gain was far reduced with two antenna diversity, the improvement in error performance was still within acceptable range. This fact has been validated by the BER comparison with the VSF scheme: namely, the MD multicode DS-CDMA can provide higher data rates while maintaining the link quality more reliably.

Appendix A
Evaluation of the Output Per-Symbol SIR γ

To begin with (12), the kth user interference $\mathrm{MAI}_k(i,e)$ can be formulated as

$$\mathrm{MAI}_k(i,e) = \frac{1}{JN}\sum_{v=1}^{V}\sum_{v'=1}^{V}\mathrm{Re}\Bigg\{\beta_{1,v}^{*}\beta_{k,v'}\varepsilon \cdot\sum_{g=0}^{G-1}\sum_{l=0}^{M-1}\left(\alpha_i \mathbf{w}_{\langle m\rangle,l}\right)\Gamma_k(g,l;n) \cdot c_{I,nN+gM+l}h_{e,g}\Bigg\} \tag{26}$$

where $\mathbf{w}_{m,l} \triangleq (w_{m,l},\ldots,w_{m+J-1,l})^T$, T denotes the transpose, and the complex-valued partial correlation function $\Gamma_k(g,l;n)$ is defined by

$$\Gamma_k(g,l;n) = a^{(k)}_{nN+gM+l-1-\nu_{k,v'}}\bar{\eta}(\delta_{k,v'}) + a^{(k)}_{nN+gM+l-\nu_{k,v'}}\bar{\eta}(T_c-\delta_{k,v'}). \tag{27}$$

Here, $a_l^{(k)} = a_{I,l}^{(k)} + j a_{Q,l}^{(k)}$, $\nu_{k,v'} = \lfloor(\tau_{k,v'}-\tau_{k,v})/T_c\rfloor$ and $\delta_{k,v'} = \tau_{k,v'} - \tau_{k,v} - \nu_{k,v'}T_c$.

Similarly, the SI $\mathrm{MAI}_{1,v}^{(O)}(i,e)$ $(O=I,Q)$ can be of the form

$$\mathrm{MAI}_{1,v}^{(O)}(i,e) = \frac{1}{JN}\sum_{\substack{v'=1\\v'\neq v}}^{V}\mathrm{Re}\Bigg\{\beta_{1,v}^{*}\beta_{1,v'} \cdot\sum_{g=0}^{G-1}\sum_{l=0}^{M-1}\left(\alpha_i \mathbf{w}_{\langle m\rangle,l}\right)\Gamma_1^{(O)}(g,l;n) \cdot c_{I,nN+gM+l}h_{e,g}\Bigg\} \tag{28}$$

in which the partial correlation function $\Gamma_1^{(O)}(g,l;n)$ becomes

$$\Gamma_1^{(O)}(g,l;n) = \exp(j\theta)[\lambda_O(g,l-1;n)\bar{\eta}(\delta_{1,v'}) + \lambda_O(g,l;n)\bar{\eta}(T_c-\delta_{1,v'})] \tag{29}$$

for $\theta = 0, \pi/2$ $(O=I,Q)$, and the multicode signal $\lambda_O(g,l;n)$ is defined by

$$\begin{aligned}\lambda_O(g,l;n) &= \sum_{m=0}^{M-1} d_{O,m}(n+\kappa_{g,l})w_{m,[(g-\kappa_{g,l}G)M+l-\nu_{1,v'}]} \\ &\quad\cdot b_{O,\langle m\rangle}(\lfloor((g-\kappa_{g,l}G)M+l-\nu_{1,v'})/M\rfloor;n+\kappa_{g,l}) \\ &\quad\cdot c_{O,nN+gM+l-\nu_{1,v'}}\end{aligned} \tag{30}$$

for $\kappa_{g,l} = \lfloor(gM+l-\nu_{1,v'})/N\rfloor$ and $[l] = l \bmod M$.

Now, the second-moment $\mathbf{E}\{\mathrm{MAI}_k^2(i,e)\}$ is evaluated as

$$\mathbf{E}\left\{\mathrm{MAI}_k^2(i,e)\right\} = \frac{V}{2JN}\left(\sum_{v=1}^{V}|\beta_{1,v}|^2\right)\sigma_\beta^2\varepsilon^2 \cdot\mathbf{E}\{\Gamma_k(g,l;n)\Gamma_k(g,l;n)^*\} \tag{31}$$

because of $\mathbf{E}\{(\alpha_i\mathbf{w}_{\langle m\rangle,l})^2\} = J$ and the random binary sequences $\{a_{O,l}^{(k)}\}$ assumed. Using $\mathbf{E}\{\Gamma_k(g,l;n)\Gamma_k(g,l;n)^*\} = 4\mathbf{E}\{\bar{\eta}^2(\delta)\}$, it follows that

$$\mathbf{E}\left\{\mathrm{MAI}_k^2(i,e)\right\} = \frac{2V}{JN}\left(\sum_{v=1}^{V}|\beta_{1,v}|^2\right)\sigma_\beta^2\varepsilon^2\mathbf{E}\{\bar{\eta}^2(\delta)\}. \tag{32}$$

Proceeding to the second-moment $\mathbf{E}\{[\mathrm{MAI}_{1,v}^{(O)}(i,e)]^2\}$ yields

$$\mathbf{E}\left\{\left[\mathrm{MAI}_{1,v}^{(O)}(i,e)\right]^2\right\} = \frac{(V-1)}{2JN}|\beta_{1,v}|^2\sigma_\beta^2 \cdot\mathbf{E}\left\{\Gamma_1^{(O)}(g,l;n)\Gamma_1^{(O)}(g,l;n)^*\right\}. \tag{33}$$

Since $\mathbf{E}\{\Gamma_1^{(O)}(g,l;n)\Gamma_1^{(O)}(g,l;n)^*\} = 2M\mathbf{E}\{\bar{\eta}^2(\delta)\}$, it is evaluated as

$$\mathbf{E}\left\{\left[\mathrm{MAI}_{1,v}^{(O)}(i,e)\right]^2\right\} = \frac{M(V-1)}{JN}|\beta_{1,v}|^2\sigma_\beta^2\mathbf{E}\{\bar{\eta}^2(\delta)\} \tag{34}$$

where we have used $\mathbf{E}\{\lambda_O^2(g,l;n)\} = M$.

Then, the total interference power σ_I^2 is

$$\sigma_I^2 = \frac{2}{JN}\left(\sum_{v=1}^{V}|\beta_{1,v}|^2\right)\sigma_\beta^2[(K-1)V\varepsilon^2 + M(V-1)]\mathbf{E}\{\bar{\eta}^2(\delta)\} \tag{35}$$

which gives the output *per-symbol* SIR as $\gamma \triangleq (\sum_{v=1}^{V}|\beta_{1,v}|^2)^2/\sigma_I^2$ in (16).

Based on the above derivations, the second-moments associated with (i,e) and (i',e') are evaluated as

$$\mathbf{E}\{\mathrm{MAI}_k(i,e)\mathrm{MAI}_k(i',e')\} = \frac{1}{JG}\left(\alpha_i\cdot(\alpha_{i'})^T\right)\cdot\left(\mathbf{h}_e\cdot(\mathbf{h}_{e'})^T\right)\mathbf{E}\left\{\mathrm{MAI}_k^2(i,e)\right\} \tag{36}$$

$$\mathbf{E}\left\{\mathrm{MAI}_{1,v}^{(O)}(i,e)\,\mathrm{MAI}_{1,v}^{(O)}(i',e')\right\} = \frac{1}{JG}\left(\alpha_i\cdot(\alpha_{i'})^T\right)\cdot\left(\mathbf{h}_e\cdot(\mathbf{h}_{e'})^T\right)\mathbf{E}\left\{\left[\mathrm{MAI}_{1,v}^{(O)}(i,e)\right]^2\right\} \tag{37}$$

which implies covar$[\rho_{\langle m\rangle}(n;i,e),\rho_{\langle m\rangle}(n;i',e')] = 1/(JG)$ $[\alpha_i\cdot(\alpha_{i'})^T][\mathbf{h}_e\cdot(\mathbf{h}_{e'})^T]\sigma_I^2$, namely, uncorrelated if $(i,e)\neq(i',e')$.

On the other hand, if the SIC is used to reduce σ_I^2, the event S will assure that $\sigma_I^2-\sum_{v=1}^{V}\mathbf{E}\{[\mathrm{MAI}_{1,v}^{(O)}(i,e)]^2\}$, leading to γ_- in (17). Otherwise, if the event $\bar{S}$ occurs, the SI is corrupted by $\widehat{\mathrm{MAI}}_{1,v}^{(O)}(i,e)$ at the vth path, where $\widehat{\ }$ denotes the estimation. The effect of incorrect SIC can be measured in the mean-square sense, i.e.,

$$\mathbf{E}\left\{\left[\mathrm{MAI}_{1,v}^{(O)}(i,e)-\widehat{\mathrm{MAI}}_{1,v}^{(O)}(i,e)\right]^2\right\} = 2\mathbf{E}\left\{\left[\mathrm{MAI}_{1,v}^{(O)}(i,e)\right]^2\right\} \tag{38}$$

since $\mathbf{E}\{\mathrm{MAI}_{1,v}^{(O)}(i,e)\widehat{\mathrm{MAI}}_{1,v}^{(O)}(i,e)\} = 0$, provided most decision errors are orthogonal to their correct ones. This implies that the penalty of incorrect SIC is equivalent to $\sigma_I^2+\sum_{v=1}^{V}\mathbf{E}\{[\mathrm{MAI}_{1,v}^{(O)}(i,e)]^2\}$, leading to γ_+ in (18).

Appendix B
Proof of Proposition 1

Let us define

$$E \triangleq \bigcup_{(i',e')\neq(i,e)}\left\{\left|\rho_{\langle m\rangle}(n;i',e')\right|>\rho_{\langle m\rangle}(n;i,e)\right\}$$

$$C_- \triangleq \bigcap_{(i',e')\neq(i,e)}\left\{\left|\rho_{\langle m\rangle}(n;i',e')-\sum_{v=1}^{V}\mathrm{MAI}_{1,v}^{(O)}(i',e')\right| < \rho_{\langle m\rangle}(n;i,e)-\sum_{v=1}^{V}\mathrm{MAI}_{1,v}^{(O)}(i,e)\right\}.$$

Using the complement $\bar{E}\triangleq C$, we have

$$P(\epsilon\to c\,|\,S) = \Pr[E;C_-\,|\,\alpha_i,\mathbf{h}_e] = \Pr[C_-\,|\,\alpha_i,\mathbf{h}_e]-\Pr[C;C_-\,|\,\alpha_i,\mathbf{h}_e] \tag{39}$$

which is equivalent to (19).

Define $\rho_{\langle m\rangle}(n;i,e)-\xi(i,e)\triangleq\rho(i,e)$ and $\sum_{v=1}^{V}\mathrm{MAI}_{1,v}^{(O)}(i,e)\triangleq\xi(i,e)$, and the second term in (39) is expressed by (40), shown at the bottom of the page. After a few steps, conditioned on $[\rho(i,e),\xi(i,e)]$ where $\rho(i,e)\geq 0$ and $\rho(i,e)+\xi(i,e)\geq 0$, it can be evaluated as

$$\begin{aligned}\Pr[\rho>\max\{|\rho(i',e')|,|\rho(i',e')+\xi(i',e')|-\xi\}\,|\,\alpha_i,\mathbf{h}_e;\ \rho(i,e)=\rho,\xi(i,e)=\xi] &= \int_0^{\rho}\frac{2}{\sigma_{I,o}}\phi\left(\frac{u}{\sigma_{I,o}}\right)\left[\int_{\max(-u,\xi)}^{-u+\rho+\xi}\frac{1}{\sigma_{I,s}}\phi\left(\frac{v}{\sigma_{I,s}}\right)dv\right.\\ &\quad\left.+\int_{-u-\rho-\xi}^{\min(-u,-2u-\xi)}\frac{1}{\sigma_{I,s}}\phi\left(\frac{v}{\sigma_{I,s}}\right)dv\right]du\\ &\quad+\int_{\max(0,-\xi)}^{\rho}\frac{2}{\sigma_{I,o}}\phi\left(\frac{u}{\sigma_{I,o}}\right)\\ &\quad\cdot\left[\int_{-2u-\xi}^{\xi}\frac{1}{\sigma_{I,s}}\phi\left(\frac{v}{\sigma_{I,s}}\right)dv\right]du\end{aligned} \tag{41}$$

where $\sigma_{I,o}^2=\sigma_I^2-\sigma_{I,s}^2$ and $\sigma_{I,s}^2=\mathbf{E}\{\xi(i,e)^2\}$. Here, we have assumed that $\{\rho(i,e),\xi(i,e)\}$ is a set of Gaussian random variables, mutually independent as shown in Appendix A. Taking the average over $[\rho(i,e),\xi(i,e)]$ yields $P(c\to c\,|\,S_-)$ in (21).

Following the above approach, a similar relation is found in (20).

Appendix C
Proof of Proposition 2

Since the error events at the second iteration are statistically correlated with initial error events, their 'in–out' relation can be characterized via the transition formula, that is

$$\begin{aligned}P_2(\epsilon) &= P(\epsilon\to\epsilon)+P(c\to\epsilon)\\ &= P(\epsilon)-P(\epsilon\to c)+P(c\to\epsilon).\end{aligned} \tag{42}$$

Here, the transition probabilities can be based on the events $(S,\bar{S})$ at the first iteration such that

$$P(\epsilon\to c)\cong P(\epsilon\to c\,|\,S)\cdot P(c\,|\,\bar{S})+P(\epsilon\to c\,|\,\bar{S})\cdot P(\epsilon\,|\,\bar{S}) \tag{43}$$

$$P(c\to\epsilon)\cong P(c\to\epsilon\,|\,S)\cdot P(c\,|\,S)+P(c\to\epsilon\,|\,\bar{S})\cdot P(\epsilon\,|\,S). \tag{44}$$

Hence, $P_2(\epsilon)$ can be derived as (22) where $P(\epsilon\to c\,|\,\bar{S})$ and $P(c\to\epsilon\,|\,S)$ are defined and derived as in Proposition 1.

$$\Pr[C;C_-\,|\,\alpha_i,\mathbf{h}_e]=\Pr\left[\bigcap_{(i',e')\neq(i,e)}\rho(i,e)>\max\{|\rho(i',e')|,|\rho(i',e')+\xi(i',e')|-\xi(i,e)\}\,|\,\alpha_i,\mathbf{h}_e\right]. \tag{40}$$

REFERENCES

[1] F. Adachi, M. Sawahashi, and H. Suda, "Wideband DS-CDMA for next-generation mobile communications system," *IEEE Commun. Mag.*, vol. 36, pp. 56–69, Sept. 1998.

[2] E. Dahlman *et al.*, "UMTS/IMT-2000 based on wideband CDMA," *IEEE Commun. Mag.*, vol. 36, pp. 70–80, Sept. 1998.

[3] I. Chih-Lin and R. D. Gitlin, "Multi-code CDMA wireless personal communications networks," in *Proc. IEEE ICC'95*, vol. 2/3, Seattle, WA, June 1995, pp. 1060–1064.

[4] I. Chih-Lin, G. P. Pollini, L. Ozarow, and R. D. Gitlin, "Performance of multi-code CDMA wireless personal communications networks," in *Proc. IEEE VTC'95*, Apr. 1995, pp. 907–911.

[5] T. Ottosson, "Precoding for minimization of envelope variations in multi-code DS-CDMA systems," IEEE Trans. Commun., submitted for publication.

[6] T. Wada, T. Yamazato, M. Katayama, and A. Ogawa, "A constant amplitude coding for orthogonal multi-code CDMA systems," *IEICE Trans. Fund.*, vol. E80-A, pp. 2477–2484, Dec. 1997.

[7] D. I. Kim, "Multidimensional constant envelope signaling for high rate multicode DS-CDMA," IEEE Trans. Commun., submitted for publication.

[8] A. J. Viterbi, "Very low rate convolutional codes for maximum theoretical performance of spread-spectrum multiple-access channel," *IEEE J. Select. Areas Commun.*, vol. 8, pp. 641–649, May 1990.

[9] S. Verdú, *Multiuser Detection*. New York: Cambridge Univ. Press, 1988.

[10] J. H. Winters, J. Salz, and R. D. Gitlin, "The impact of antenna diversity on the capacity of wireless communications systems," *IEEE Trans. Commun.*, vol. 42, pp. 1740–1750, Feb./Mar./Apr. 1994.

[11] S. Tanaka, A. Harada, M. Sawahashi, and F. Adachi, "Experiments on coherent antenna array diversity for wideband CDMA mobile radio," in *Proc. IEEE VTC'99*, vol. 1/3, May 1999, pp. 243–248.

[12] J. M. Wozencraft and I. M. Jacobs, *Principles of Communication Engineering*. New York: Wiley, 1965.

[13] S. B. Wicker, *Error Control Systems for Digital Communication and Storage*. Englewood Cliffs, NJ: Prentice-Hall, 1995.

[14] R. K. Morrow and J. S. Lehnert, "Bit-to-bit dependence in slotted DS/SSMA packet system with random signature sequences," *IEEE Trans. Commun.*, vol. 37, pp. 1052–1061, Oct. 1989.

[15] V. Tarokh, N. Seshadri, and A. R. Calderbank, "Space-time codes for high data rate wireless communication: Performance analysis and code construction," *IEEE Trans. Inform. Theory*, vol. 44, pp. 744–765, Mar. 1998.

Dong In Kim (S'89–M'91) received the B.S. and M.S. degrees in electronics engineering from Seoul National University, Seoul, Korea, in 1980 and 1984, respectively, and the M.S. and Ph.D. degrees in electrical engineering from the University of Southern California (USC), Los Angeles, in 1987 and 1990, respectively.

From 1984 to 1985, he was with the Korea Telecommunication Research Center as a Researcher. During 1986–1988, he was a Korean Government Graduate Fellow in the Department of Electrical Engineering, USC. From 1988 to 1990, he was a Research Assistant at the USC Communication Sciences Institute. Since 1991, he has been with the University of Seoul, Seoul, Korea, where he is currently an Associate Professor at the School of Electrical Engineering, leading the Wireless Communications Research Group. He was a Visiting Professor at the University of Victoria, Victoria, BC, Canada, during 1999–2000. He has given many short courses and lectures on the topics of spread-spectrum and wireless communications at several companies. He has performed research in the areas of packet radio networks and spread-spectrum systems since 1988. His current research interests include spread-spectrum systems, cellular mobile communications, indoor wireless communications, and wireless multimedia networks.

Dr. Kim is currently a Division Editor of the *Journal of Communications and Networks*.

Vijay K. Bhargava (S'70–M'74–SM'82–F'92) received the B.Sc., M.Sc., and Ph.D. degrees from Queen's University, Kingston, ON, Canada, in 1970, 1972, and 1974, respectively.

He is a Professor of Electrical and Computer Engineering at the University of Victoria, Victoria, BC, Canada, and is currently spending a sabbatical year at the Hong Kong University of Science and Technology. He is a co-author of the book *Digital Communications By Satellite* (New York: Wiley, 1981) and co-editor of the IEEE Press Book *Reed–Solomon Codes and Their Applications*. His research interests include multimedia wireless communications.

Dr. Bhargava is a Fellow of the B.C. Advanced Systems Institute, Engineering Institute of Canada (EIC), the IEEE and the Royal Society of Canada. He is an Editor-in-Chief of W*ireless Personal Communication*, a Kluwer Periodical. Dr. Bhargava is very active in the IEEE and is currently the President of the IEEE Information Theory Society. He was Co-Chair for IEEE ISIT'95, Technical Program Chair for IEEE ICC'99, and is the Chair of IEEE VTC'2002 Fall to be held in Vancouver, BC, Canada. He is a recipient of the IEEE Centennial Medal (1984), IEEE Canada's McNaughton Gold Medal (1995), the IEEE Haraden Pratt Award (1999), and the IEEE Third Millennium Medal (2000).